Two-photon absorption by a quantum dot pair

Michael Scheibner, Sophia E. Economou, Ilya V. Ponomarev, Cameron Jennings, Allan S. Bracker, and Daniel Gammon

Phys. Rev. B **92**, 081411 — Published 31 August 2015

DOI: 10.1103/PhysRevB.92.081411

Two-Photon Absorption by a Quantum Dot Pair

Michael Scheibner,[1,*] Sophia E. Economou,[2] Ilya V. Ponomarev,[3]
Cameron Jennings,[1] Allan S. Bracker,[2] and Daniel Gammon[2]

[1] *University of California Merced, 5200 North Lake Road, Merced, California 95343, USA*
[2] *Naval Research Laboratory, 4555 Overlook Avenue, SW, Washington, D.C. 20375, USA*
[3] *Thomson Reuters, 1455 Research Boulevard, Rockville, Maryland 20850, USA*[†]

The biexciton absorption spectrum of a pair of InAs/GaAs quantum dots is being studied by photoluminescence excitation spectroscopy. An absorption resonance with the characteristics of an instantaneous two-photon process reveals a coherent interdot two-photon transition. Pauli-selective tunneling is being used to demonstrate the transduction of the two-photon coherence into a non-local spin singlet state. The two-photon transition can be tuned spectrally by electric field, enabling amplification of its transition strength.

PACS numbers: 78.67.Hc, 78.47.jh, 78.55.Cr, 78.30.-j

Two-photon excitation of a single quantum dot (QD), finds broad use across disciplines, ranging from fundamental quantum mechanics, such as in the measurement, control and entanglement of the exciton-spin qubit[1–3], to biomedical imaging[4]. Most commonly, the cascade-type energy level diagram of the biexciton in a QD is considered a natural source of (heralded) single photons, and two correlated or even entangled photons[5–8]. In connection to scalability and quantum networks, efforts have been spent on two-photon interference from disparate single photon sources, such as two QDs[9,10], as well as realizing large-scale arrays of QD entangled photon sources. For on-chip information processing, communication and conversion to and from other information carriers, both, absorption and emission are needed.

The coupling of a second QD to the first through coherent tunneling[11–13] has initiated a development through which a steadily increasing number of advantages for quantum optics applications are currently being revealed. For example, the lifetime of the exciton when used as a qubit can be greatly enhanced by separating the electron and hole to the two QDs[14]. For two-photon emission, the anisotropic exchange interaction that frustrates entanglement can be greatly reduced and may even be eliminated by separating the particles[15,16]. Further, the rich energy level and transition spectrum of coupled quantum dots (CQDs) has been shown to allow for implementing conditional dynamics of the light-matter interaction[17]. Although the level diagram of the biexciton cascade in CQDs has been measured using photoluminescence spectroscopy[18], little is known about the coherent properties of the molecular biexciton to this point.

Here we present frequency-domain resonant excitation spectroscopy of the molecular biexciton in a CQD pair[18]. We reveal two-photon transitions by which the molecular biexciton is directly and coherently generated. We demonstrate that a two-photon transition involving both dots exists and that it transduces into a spin singlet state of the dot pair, i.e., the two dots are being spin-entangled. Moreover, the strength of the transition is tunable by an applied electric field. Hence implementations of two-photon quantum protocols in integrated solid state device architectures are being enabled. For example, Zeno-type conditional coherent logic down to the single photon level becomes feasible in a monolithic nanoscale system[19–22]. Furthermore, charge redistribution or removal could be used to tune the lifetime of the optically-induced entangled state or to convert the optical entanglement into a hybrid or pure particle entanglement, resulting in potential quantum memory technology for single and entangled photons[14,23–27] as well as opening additional paths for spin-photon entanglement[28,29]. The spin selectivity of the two-photon transition provides the means to optically initiate the system in a spin singlet state even if the singlet-triplet splitting is spectrally not resolvable. Such a capability is useful for interfacing spin with other energetically small quanta of information such as, for example, phononic (quantum) information[30–33]. The interdot nature of the revealed two-photon transition could provide scalability of any enabled processes to

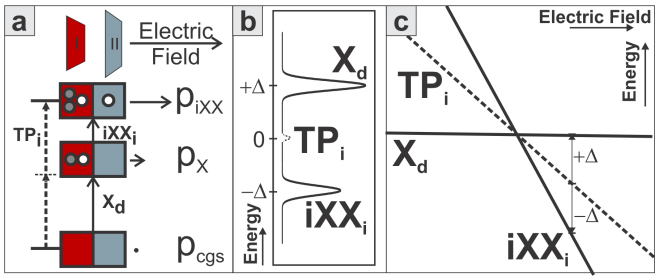

FIG. 1. (a) Top: Sample geometry with the dot color indicating the relative bandgap energy of the two dots (left, red → lower bandgap, right, blue → higher bandgap). Bottom: Energy level diagram with resonant optical single-photon, X_d and iXX_i, and monochromatic two-photon, TP_i, transitions between the crystal ground state(cgs), exciton (X) and molecular biexciton (iXX). The static dipole moments of the different states, p_{cgs}, p_X, and p_{iXX}, are illustrated. (b) Schematic exciton-biexciton transition spectrum with single and two-photon transitions. (c) Predicted EFD absorption spectrum from a CQD pair for the states and transitions depicted in a.

extended dot systems.

The CQDs used in this study consist of two 2.5nm Stranski-Krastanov type InAs/GaAs QDs fabricated by molecular beam epitaxy. The QDs were separated by a 6nm (4nm) GaAs barrier and embedded within the 371nm wide intrinsic region of a n-type Schottky-diode structure. The detailed structure has been reported in ref.[34]. Even though the dots in both layers are nominally of the same height, the top dots are commonly found to exhibit a higher bandgap[35]. Hence we refer to them as red (low energy) and blue (high energy) dots (Fig. 1a). By applying electrical bias to the diode structure we create an electric field along the axis of the dot pair. Thereby we Stark-shift the QD electronic energy levels and optical transitions due to the dipole moments of the involved states (Fig. 1a-c) and enable hole level resonances between the dots[36]. The sample was mounted and electrically contacted inside a ceramic chip header, which was mounted on the cold finger of a continuous flow cryostat and kept at a temperature of 15 K.

The QDs were optically excited with a continuous wave titanium sapphire laser, with a bandwidth of less than 1 GHz and an excitation power density of $40\mu W/\mu m^2$. Photoluminescence (PL) was spectrally dispersed with a triple 0.75m Raman spectrometer, where each stage was equipped with a $1200mm^{-1}$ grating. The spectrometer was operated in subtractive mode (Raman mode) unless otherwise noted. The spectrally dispersed PL was collected with a liquid nitrogen cooled charge coupled device (CCD) camera, yielding an overall PL spectral resolution of $50\mu eV$. PL spectra were recorded as function of electric bias applied to the diode structure. In order to measure the biexciton absorbtion spectrum of a CQD pair we create electric field dispersed (EFD) PL excitation (PLE) spectra (see Fig.2a&b). To generate these PLE spectra, EFD-PL spectra were recorded at various excitation energies[37]. The intensity of selected PL lines was monitored and summed spectrally for each of these PL spectra and combined to create PLE (absorption) spectra as function of electric field (Fig.2b top)[30]. Enhanced PL intensity from the monitored PL line indicates enhanced absorption due to resonance of the laser with a transition. The use of the spectrometer in Raman mode allowed for measuring PL transitions of a single CQD pair with the laser excitation tuned as close as 0.5 meV to the detected transitions.

Here we limit the discussion to CQD states with all charges in the red dot and at most one hole in the blue dot, which we will refer to as single dot-like (SQD-like) and molecular respectively[38]. In either case the charges only occupy the electronic ground state levels of the dots. From here on we use X to represent a SQD-like exciton, iX a molecular exciton, and consequently XX a SQD-like biexciton and iXX a molecular biexciton (1 X & 1 iX). Absorption (emission) transitions are labeled by their final (initial) state with subscripts "d" or "i" identifying the transitions as spatially direct or indirect respectively.

A two-photon transition, TP, as indicated in Fig.1b, can be found in absorption spectra in addition to the exciton, X, and biexciton, XX, single-photon transitions. For a monochromatic excitation the two-photon transition is spectrally centered between the exciton and biexciton transitions at energies $\pm\Delta$ as follows from the level diagram in Fig.1a. CQDs provide the potential to tune the transition energies with electric field if one of the involved states is spatially indirect and possesses a large electric dipole moment (Fig.1a). The energy shift of an absorption transition, ΔE, due to electric field tuning, $\Delta\mathbf{F}$, scales with the electric dipole moments of the initial and the final state of the transition, $\mathbf{p}_i$ and $\mathbf{p}_f$ respectively, and the number, N, of photons involved in the transition as $\Delta E = \Delta\mathbf{F}(\mathbf{p}_f - \mathbf{p}_i)/N$[39,40]. For transitions depicted in Fig.1a&b the EFD absorption spectrum of Fig.1c can be predicted. In the following we will experimentally reveal this interdot two-photon transition and determine the spin state of the generated biexciton.

While single-photon transitions can be seen easily in PL[18], the coherent two-photon transitions only become visible in absorption. Figure 2b shows a combined EFD-PL/PLE spectrum of the biexciton-exciton transitions of a CQD pair. The bottom part displays biexciton single photon PL transitions after excitation at the energy marked by the arrow for the $TP_{d/i}$ label. The top part

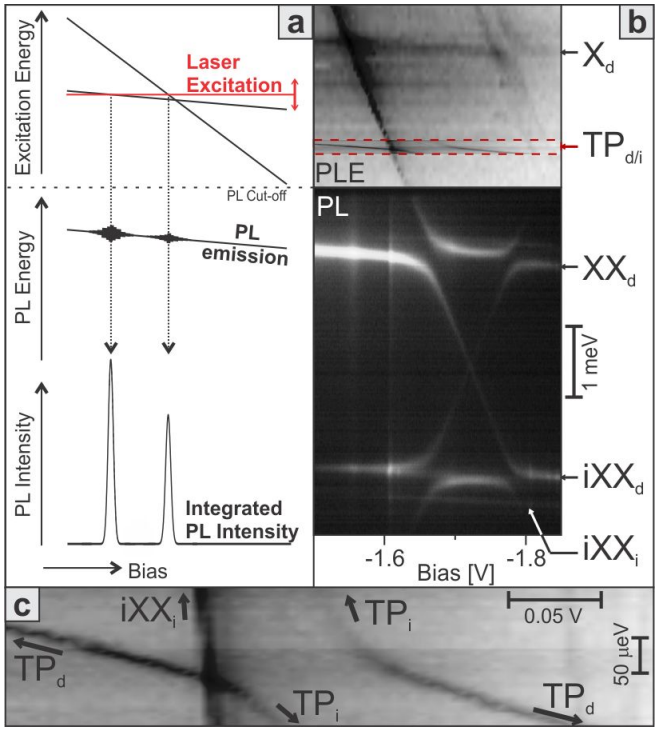

FIG. 2. (a) Illustration of the generation of an EFD-PLE absorption spectrum. (b) Combined EFD-PL (bottom) and PLE (top) spectrum. The PL spectrum was obtained at the energy marked by the arrow for the $TP_{d/i}$ label. The region in the dashed box was taken with 10 times smaller energy steps than the rest. (c) Expanded view of the region in the dashed box in b.

was constructed from several such PL spectra obtained at different excitation energies, by summing the PL intensity from the XX_d and iXX_d biexciton transitions. Together both parts show most lines that are commonly observed in PL under non-resonant excitation. In addition, the SQD-like coherent two-photon transition, TP_d, is found midway between the X_d and the XX_d transitions (dashed red box). This region is shown in detail in Fig.2c, which reveals that the TP_d transition undergoes an anticrossing with another two-photon transition, TP_i. It is important to note that information from both biexciton configurations, XX and iXX, is obtained in one and the same measurement. It should further be noted, that a small probability for creating excitons and biexcitons exists also if the excitation is not strictly resonant with the respective transitions, due to phonon-assisted processes. These processes can be suppressed and the two-photon absorption optimized by lowering the temperature and by using chirped pulsed excitation[41,42], yet here they come in handy for the identification of the observed transitions.

To uncover the full nature of the two-photon transitions we will utilize the fine structure of CQDs.[18,34] As tools for this purpose we use the following fine structure features: 1. anticrossings due to tunnel coupling at level resonances, 2. electron-hole exchange splitting, δ_{BD}, between bright and dark exciton states and 3. singlet-triplet kinetic exchange splitting, δ_{ST}, at tunnel resonances where two like spins are involved[18,34]. Combined with an anticrossing either type of exchange splitting varies characteristically in magnitude as one follows either the two branches of the anticrossing (Fig.3a&b). To utilize these features as tools we briefly recall their characteristics.

The singlet-triplet splitting is caused by the interplay of tunnel coupling and Pauli exclusion principle. While tunneling into the orbital ground state of the same dot is allowed for two holes in a spin singlet state, it is forbidden by the Pauli exclusion principle if they are in either of the three triplet states (Fig.3a)[35,43–45]. The resulting signature, an anticrossing with a straight line through the center, is found in PL transitions that map the hole level resonance of the XX and iXX states[18,34]. An example is the bottom left anticrossing of the biexciton X-pattern (Figs.2b & 3c), which is caused by the biexciton transitions into the iX state. Besides the Pauli exclusion of SQD-like ground state spin triplets this anticrossing shows that the iXX triplet states are optically active. Hence tunneling into the SQD-like biexciton provides a filter mechanism, which can be read out by PL.

Another tool for identifying the iXX spin states is the electron-hole exchange splitting, δ_{BD}, between the bright and dark exciton states. Provided that the z-component of the angular momentum, J_z, is conserved, optical transitions connect the T±3 triplet states with the dark exciton states only and the singlet and the T0 triplet iXX states with the bright exciton states only. The bright-dark splitting in the iX states is reduced far

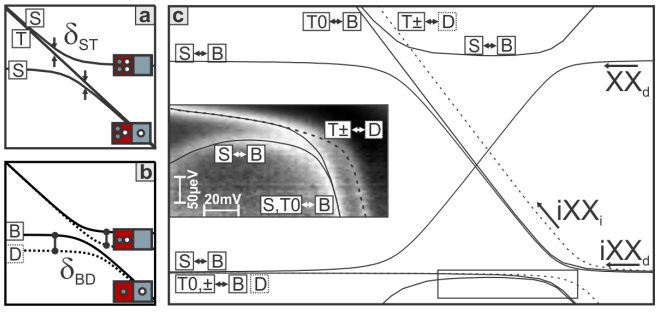

FIG. 3. (a) Fine structure of the biexciton level resonance and (b) the exciton level resonance. The singlet-triplet splitting, δ_{ST}, and the bright-dark splitting, δ_{BD}, are marked in both branches of the respective anticrossings. (c) Schematic EFD biexciton transition spectrum with transitions labeled by the exciton and biexciton spin states. Inset: High-resolution EFD-PL spectrum of the boxed region of the biexciton X-pattern. This spectrum was obtained with the triple spectrometer in additive mode under non-resonant excitation at 1.374eV. The intensity was normalized at each energy. The lines are guide to the eye.

below the PL resolution and hence not seen in the iXX_d PL transitions[18,34] (3b&c). Yet where the $iXX_{d/i}$ transitions map the hole level resonance of the neutral exciton the bright-dark splitting of the SQD-like exciton emerges in the optical spectrum. There the increasing δ_{BD} splits the iXX_i transitions involving the T±3 triplet states from the iXX_i transitions involving the T0-triple state (Fig.3c inset). Away from the iXX-XX resonance the T0-iXX_i transition is asymptotically joined by the iXX_i transition involving the iXX singlet state (see also[46]).

The two-photon transition into the biexciton must also map the iXX-XX level resonance and exhibit an anticrossing. An anticrossing is indeed observed (Fig.2c). The anticrossing splitting measures half the value as seen in PL, which is consistent with the fact that two photons instead of one photon partake in the optical transition. In contrast to what is seen in PL the two-photon transitions do not appear to show the signature of the three triplet states. The straight line that can be seen in Fig. 2c is the iXX_i single-photon transition. The absence of the triplet feature could be caused by the typical weakness of interdot transitions or fundamental selection rules.

The interdot two-photon transition TP_i, can be expected to be strongest at the resonance of the intradot neutral exciton transition, X_d, and the interdot biexciton transition, iXX_i. This fact shows in the PLE spectra of Figs.4a & b. In Fig. 4a we find the TP_i transition to reach about 25% the peak intensity of the iXX_i transition before they overlap. Here we took advantage of monitoring the XX_d and iXX_d transitions separately, enabling an analysis of the spin states involved in the various transitions. Absorption transitions into the iXX singlet *and* triplet states are made visible by monitoring the iXX_d PL transitions (Figs.3c & 4b). In contrast, none of the iXX spin triplet configurations that may have been cre-

ated are detected via the XX_d transition (Figs.3c & 4a), as the relaxation into the SQD-like biexciton acts as a spin filter.

The distribution of spin levels (Fig.4c) and conservation of J_z under optical excitation yield two spin fine structure features in the absorption spectra. First, any residual singlet-triplet splitting, δ_{ST}, should be visible as difference between the single-photon transitions from the bright exciton states into the singlet and T0-triplet iXX states. Second, the electron-hole spin exchange splitting of the SQD-like exciton, δ_{BD}, should be visible as difference between the transition from the bright X states (B±) to the T0-triplet iXX state and the transitions from the dark X states (D±) to the T±-triplet iXX states.

The comparison of Figs.4a & b together with the spin level structure of Fig.4c identify the second higher energy iXX_i transition in Fig. 4b as a single-photon transition originating from a dark intradot exciton ($J_z = \pm 2$) to the molecular biexciton T± hole spin triplets ($J_z = \pm 3$). A closer look, using the yellow markers in Figs.4a & b, further reveals that the stronger iXX_i transition gains some spectral width in Fig.4b. With both data sets originating from one and the same measurement and the gain in width being one-sided, spectral diffusion and power broadening can be excluded as cause. Instead, this additional width can be attributed to a transition from the bright exciton ($J_z = \pm 1$) into the T0 hole spin triplet ($J_z = 0$). The same detailed graphical analysis shows that the TP_i transition does not exhibit any change in

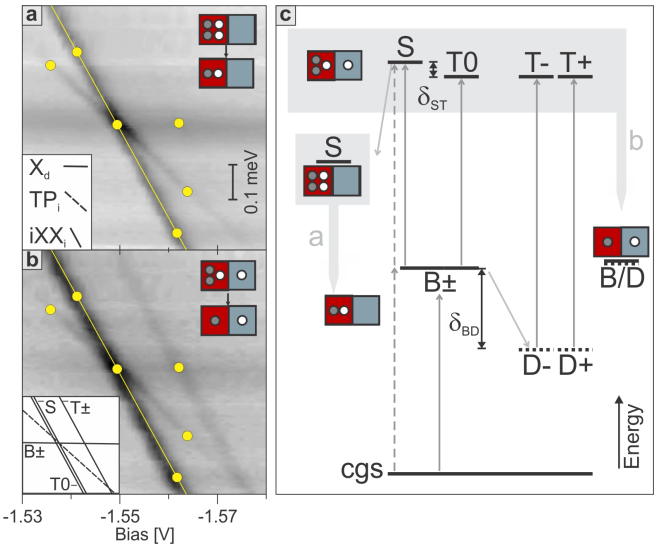

FIG. 4. EFD-PLE absorption spectra in the vicinity of the resonance of the X_d and iXX_i transitions obtained by monitoring (a) the XX_d and (b) the iXX_d PL transitions. Yellow markers are placed in the exact same positions in (a) and (b). Inset to (b): Summary of all transitions; identified by the spin states they generate.(c) Energy level structure of the exciton-biexciton system at a fixed bias in the region seen in (a) and (b). Thin arrows indicate the excitation paths, wide grey arrows the detection transitions used in (a) and (b).

width or spectral position. Thus we can conclude that the two-photon excitation exclusively generates spin singlet states, that is, it creates a spin entangled state of the two dots. The inset to Fig. 4b summarizes this experimental evidence, identifying the various transitions by the spin states they generate.

Second order time-dependent perturbation treatment of this two-photon absorption supports the finding that triplet state transitions are prohibited, as long as no spin mixing between singlet and triplet states exists[46]. Without singlet-triplet mixing, only bright-dark mixing or spin-flip inducing time evolution of the intermediate exciton spin state could allow for the optical generation of the triplet states, which is possible for the sequential single-photon transitions. In contrast, the two-photon transition, TP_i, must be instantaneous and thereby bypassing the exciton states.

In conclusion, we have shown that an interdot two-photon transition, TP_i, exists and that it generates a non-local spin singlet. For this proof a resonance region (see Fig.4a/b) was chosen that allowed for the spectral separation of the various transitions and the utilization of spin selective tunneling to identify the transitions by the exciton and biexciton spin states they optically connect. However, with the TP_i transition the singlet state can be optically selected even if the singlet-triplet splitting is optically not resolvable with single-photon transitions.

* mscheibner@ucmerced.edu

† Now at: Euclid Techlabs, 400 Professional Drive, Gaithers-

burg MD 20879
[1] K. Brunner, G. Abstreiter, G. Böhm, G. Tränkle, and G. Weimann, Phys. Rev. Lett. **73**, 1138 (1994).
[2] X. Li, Y. Wu, D. Steel, D. Gammon, T. H. Stievater, D. S. Katzer, D. Park, C. Piermarocchi, and L. J. Sham, Science **301**, 809 (2003).
[3] Y. Benny, Y. Kodriano, E. Poem, S. Khatsevitch, D. Gershoni, and P. M. Petroff, Phys. Rev. B **84**, 075473 (2011).
[4] L. M. Maestro, J. E. Ramírez-Hernández, N. Bogdan, J. A. Capobianco, F. Vetrone, J. G. Soléa, and D. Jaque, Nanoscale **4**, 298 (2012).
[5] C. Santori, D. Fattal, M. Pelton, G. S. Solomon, and Y. Yamamoto, Phys. Rev. B **66**, 045308 (2002).
[6] N. Akopian, N. H. Lindner, E. Poem, Y. Berlatzky, J. Avron, D. Gershoni, B. D. Gerardot, and P. M. Petroff, Phys. Rev. Lett. **96**, 130501 (2006).
[7] R. J. Young, R. M. Stevenson, P. Atkinson, K. Cooper, D. A. Ritchie, and A. J. Shields, New Journal of Physics **8**, 29 (2006).
[8] M. Müller, S. Bounouar, K. D. Jöns, M. Glässl, and P. Michler, Nature Phot. **8**, 224 (2014).
[9] S. V. Polyakov, A. Muller, E. B. Flagg, A. Ling, N. Borjemscaia, E. V. Keuren, A. Migdall, and G. S. Solomon, Phys. Rev. Lett. **107**, 157402 (2011).
[10] R. B. Patel, A. J. Bennett, I. Farrer, C. A. Nicoll, D. A. Ritchie, and A. J. Shields, Nature Phot. **4**, 632 (2010).
[11] E. A. Stinaff, M. Scheibner, A. S. Bracker, I. V. Ponomarev, V. L. Korenev, M. E. Ware, M. F. Doty, T. L. Reinecke, and D. Gammon, Science **311**, 636 (2006).
[12] H. J. Krenner, M. Sabathil, E. C. Clark, A. Kress, D. Schuh, M. Bichler, G. Abstreiter, and J. J. Finley, Phys. Rev. Lett. **94**, 057402 (2005).
[13] G. Ortner, M. Bayer, Y. Lyanda-Geller, T. L. Reinecke, A. Kress, J. P. Reithmaier, and A. Forchel, Phys. Rev. Lett. **94**, 157401 (2005).
[14] A. B. de la Giroday, N. Sköld, R. M. Stevenson, I. Farrer, D. A. Ritchie, and A. J. Shields, Phys. Rev. Lett. **106**, 216802 (2011).
[15] H. Y. Rairez and S.-J. Cheng, Phys. Rev. Lett. **104**, 206402 (2010).
[16] N. Sköld, A. B. de la Giroday, A. J. Bennett, I. Farrer, D. A. Ritchie, and A. J. Shields, Phys. Rev. Lett. **110**, 016804 (2013).
[17] L. Robledo, J. Elzerman, G. Jundt, M. Atatüre, A. Högele, and A. I. S. Fält1, Science **320**, 772 (2008).
[18] M. Scheibner, I. V. Ponomarev, E. A. Stinaff, M. F. Doty, A. S. Bracker, C. S. Hellberg, T. L. Reinecke, and D. Gammon, Phys. Rev. Lett. **99**, 197402 (2007).
[19] J. D. Franson, B. C. Jacobs, and T. B. Pittman, Phys. Rev. A **70**, 062302 (2004).
[20] B. C. Jacobs and J. D. Franson, Phys. Rev. A **79**, 063830 (2009).
[21] L. Schneebeli, T. Feldtmann, M. Kira, S. W. Koch, and N. Peyghambarian, Phys. Rev. A **81**, 053852 (2010).
[22] K. J. Xu, Y. P. Huang, M. G. Moore, and C. Piermarocchi, Phys. Rev. Lett. **103**, 037401 (2009).
[23] M. Kroutvar, Y. Ducommun, D. Heiss, M. Bichler, D. Schuh, G. Abstreiter, and J. J. Finley, Nature **432**, 81 (2004).
[24] C. Simon, M. Afzelius, J. Appel, A. B. de la Giroday, S. J. Dewhurst, N. Gisin, C. Y. Hu, F. Jelezko, S. Kröll, J. H. Mller, J. Nunn, E. S. Polzik, J. G. Rarity, H. D. Riedmatten, W. Rosenfeld, A. J. Shields, N. Sköld, R. M. Stevenson, R. Thew, I. A. Walmsley, M. C. Weber, H. Weinfurter, J. Wrachtrup, and R. J. Young, The European Physical Journal D **58**, 1 (2010).
[25] E. Saglamyurek, N. Sinclair, J. Jin, J. A. Slater, D. Oblak, F. Bussières, M. George, R. Ricken, W. Sohler, and W. Tittel, Nature **469**, 512 (2011).
[26] H. P. Specht, C. Nölleke, A. Reiserer, M. Uphoff, E. Figueroa, S. Ritter, and G. Rempe, Nature **473**, 190 (2011).
[27] M. P. Hedges, J. J. Longdell, Y. Li, and M. J. Sellars, Nature **465**, 1052 (2010).
[28] K. D. Greve, P. L. M. L. Yu, J. S. Pelc, C. M. Natarajan, N. Y. Kim, E. Abe, S. Maier, C. Schneider, M. Kamp, S. Höfling, R. H. Hadfield, A. Forchel, M. M. Fejer, and Y. Yamamoto, Nature **491**, 421 (2012).
[29] W. B. Gao, P. Fallahi, E. Togan, J. Miguel-Sanchez, and A. Imamoglu, Nature **491**, 426 (2012).
[30] M. L. Kerfoot, A. O. Govorov, C. Czarnocki, D. Lu, Y. N. Gad, A. S. Bracker, D. Gammon, and M. Scheibner, Nature Commun. (2014), 10.1038/ncomms4299.
[31] N. Li, J. Ren, L. Wang, G. Zhang, P. Hänggi, and B. Li, Rev. Mod. Phys. **84**, 1045 (2012).
[32] S. D. Bennett, N. Y. Yao, J. Otterbach, P. Zoller, P. Rabl, and M. D. Lukin, Phys. Rev. Lett. **110**, 156402 (2013).
[33] S. R. Sklan, AIP Advances **5**, 053302 (2015).
[34] M. Scheibner, M. F. Doty, I. V. Ponomarev, A. S. Bracker, E. A. Stinaff, V. L. Korenev, T. L. Reinecke, and D. Gammon, Phys. Rev. B **75**, 245318 (2007).
[35] M. Scheibner, M. Yakes, A. S. Bracker, I. V. Ponomarev, M. F. Doty, C. S. Hellberg, L. J. Whitman, T. L. Reinecke, and D. Gammon, Nature Physics **4**, 291 (2008).
[36] A. S. Bracker, M. Scheibner, M. F. Doty, E. A. Stinaff, I. V. Ponomarev, J. C. Kim, L. J. Whitman, T. L. Reinecke, and D. Gammon, Appl. Phys. Lett. **89**, 233110 (2006).
[37] The optimal spectral and bias ranges were determined from spectra obtained under non-resonant excitation, such as shown in[46].
[38] Here spatial location is understood in terms of the relaxed limits of the quantum mechanical particle-wave dualism, which enables tunneling and the formation of interdot states due to finite wave function overlap of the particles with both dots.
[39] B. Szafran, F. M. Peeters, and S. Bednarek, Phys. Rev. B **75**, 115303 (2007).
[40] S. Ramanathan, G. Petersen, K. Wijesundara, R. Thota, E. A. Stinaff, M. L. Kerfoot, M. Scheibner, A. S. Bracker, and D. Gammon, Appl. Phys. Lett. **102**, 213101 (2013).
[41] M. Glässl, A. M. Barth, K. Gawarecki, P. Machnikowski, M. D. Croitoru, S. Lüker, D. E. Reiter, T. Kuhn, and V. M. Axt, Phys. Rev. B **87**, 085303 (2013).
[42] A. Debnath, C. Meier, B. Chatel, and T. Amand, Phys. Rev. B **88**, 201305 (2013).
[43] B. Urbaszek, R. J. Warburton, K. Karrai, B. D. Gerardot, P. M. Petroff, and J. M. Garcia, Phys. Rev. Lett. **90**, 247403 (2003).
[44] E. Poem, J. Shemesh, I. Marderfeld, D. Galushko, N. Akopian, D. Gershoni, B. D. Gerardot, A. Badolato, and P. M. Petroff, Phys. Rev. B **76**, 235304 (2007).
[45] Y. Arashida, Y. Ogawa, and F. Minami, Phys. Rev. B **85**, 235318 (2012).
[46] See supplementary information.

ACKNOWLEDGMENTS

MS and CJ acknowledge financial support from the NSF Center for Integrated Nanomechanical Systems under Grant number NSF-EEC-0832819. MS acknowledges support from the Hellman Family Faculty Foundation.